3020 *Inorg. Chem.* **1990**, *29*, 3020–3026

Contribution from the Department of Chemistry, Faculty of Science, Hiroshima University, 1-1-89 Higashi-senda-machi, Naka-ku, Hiroshima 730, Japan, and Department of Fundamental Science, Okayama University of Science, 1-1 Ridai-cho, Okayama 700, Japan

Structural Study of Optical Resolution. 14. Highly Efficient Chiral Discrimination of the *lel*$_3$-Tris(*trans*-1,2-cyclohexanediamine)cobalt(III) Ion Attained with the *d*-(*R*,*R*)-Tartrate Ion Assuming an Anomalous Conformation

Tsutomu Mizuta,[†] Kazuo Toshitani,[†] Katsuhiko Miyoshi,[*,†] and Hayami Yoneda[‡]

Received October 12, 1989

The crystal structures of the diastereomeric salt pair Λ-*lel*$_3$-[Co(*S*,*S*-chxn)$_3$]Cl(*d*-tart)·2H$_2$O (I) and Δ-*lel*$_3$-[Co(*R*,*R*-chxn)$_3$]Cl(*d*-tart)·2H$_2$O (II) (chxn = *trans*-1,2-cyclohexanediamine and *d*-tart = *d*-(*R*,*R*)-tartrate dianion) have been determined by single-crystal X-ray structure analysis. Crystal data are as follows: I is hexagonal, with space group $P6_3$, $Z = 6$, $a = b = 22.068$ (6) Å, $c = 10.492$ (2) Å, $R = 0.058$, and 2206 reflections; II is orthorhombic, with space group $P2_12_12_1$, $Z = 4$, $a = 9.666$ (3) Å, $b = 12.999$ (3) Å, $c = 22.950$ (6) Å, $R = 0.050$, and 3368 reflections. In both crystals is found a characteristic local structure in which the *d*-tart^{2-} anion directs four of its oxygen atoms toward the complex cation, with three of them hydrogen-bonded to the three amino protons that protrude almost parallel to the C_3 axis of the complex. The *d*-tart^{2-} ion in I assumes a normal conformation close to that usually found, while an unprecedented conformer is found in II, in which the distal carboxylate group is rotated greatly to avoid the steric repulsion otherwise imposed on it by one of the bulky chxn chelates of Δ-*lel*$_3$-[Co(*R*,*R*-chxn)$_3$]$^{3+}$. Ab initio molecular orbital calculations on the *d*-tart^{2-} ion reveal that rotation of the carboxylate group leads to substantial destabilization, which accounts for a large solubility difference between the two diastereomeric salts I and II and is ultimately responsible for highly efficient optical resolution attained for *lel*$_3$-[Co(chxn)$_3$]$^{3+}$ by ion-exchange chromatography with aqueous sodium *d*-tartrate as an eluent.

Introduction

Elucidating the mechanism of chiral recognition is one of the most fascinating and important subjects for planning efficient optical resolution of chiral molecules or controlling enantio- or diastereoselective reactions.[1,2]

d-Tartaric acid and its salts (and its derivatives) have been successfully utilized as resolving reagents or chiral sources in the stereoselective reactions, though they are relatively small organic molecules. Their wide utility arises not only from facile availability from natural products but also from unique structural features; they have vicinal asymmetric centers and usually assume one common and fairly stable conformation in which the four carbon atoms lie almost on the same plane, and all of the carbon and oxygen atoms in each α-hydroxy carboxylate moiety are coplanar,[3] as has been confirmed by a number of structure analyses[4] of the *d*-tartrate or hydrogen *d*-tartrate anion.

When the *d*-tartrate ion takes this unique conformation, four of its oxygen atoms, i.e., two hydroxyl and two carboxyl oxygen atoms, necessarily lie almost on the same plane, and they are chirally disposed on it. So, this "anionic" chiral face is expected to facilitate recognition of the chirality of molecules that have a "cationic" face to interact with it. Actually, the *d*-tartrate ion has been successfully used to resolve several metal amine complex cations. For example, Yoshikawa and Yamasaki[5] achieved the complete resolution of the [Co(en)$_3$]$^{3+}$ cation (en = ethylenediamine) on an SP-Sephadex cation-exchange column with aqueous sodium *d*-tartrate solution as an eluent. It is notable, however, that *lel*$_3$-[Co(chxn)$_3$]$^{3+}$ and *lel*$_3$-[Co(pn)$_3$]$^{3+}$ cations (chxn = *trans*-1,2-cyclohexanediamine and pn = 1,2-propanediamine) are much more effectively discriminated with the *d*-tartrate ion than the [Co(en)$_3$]$^{3+}$ ion is in aqueous solution,[6] though they have a similar "cationic" face consisting of three amino protons. In the present study, crystal structure analyses have been carried out on the diastereomeric salt pair Λ-*lel*$_3$-[Co(*S*,*S*-chxn)$_3$]Cl(*d*-tart)·2H$_2$O and Δ-*lel*$_3$-[Co(*R*,*R*-chxn)$_3$]Cl(*d*-tart)·2H$_2$O (*d*-tart = *d*-tartrate dianion) in order to explore the factors leading to highly efficient chiral discrimination attained for the above two *lel*$_3$ complexes. In addition, conformational energies have been estimated for the *d*-tart^{2-} ion on the basis of ab initio molecular orbital calculations, since its anomalous conformer has been found in the latter diastereomeric salt.

Experimental Section

X-ray Structure Analyses. Λ-*lel*$_3$-[Co(*S*,*S*-chxn)$_3$]Cl(*d*-tart)·2H$_2$O (I), formed on mixing Λ-*lel*$_3$-[Co(*S*,*S*-chxn)$_3$]Cl$_3$[7] with Na$_2$[*d*-tart] in water, was redissolved in water, and orange crystals were grown by slow evaporation. Orange crystals of Δ-*lel*$_3$-[Co(*R*,*R*-chxn)$_3$]Cl(*d*-tart)·2H$_2$O (II) were obtained in the same manner.[7] The crystals selected for data collection had dimensions of 0.40 × 0.40 × 0.35 and 0.48 × 0.40 × 0.25 mm for I and II, respectively. X-ray data collection was carried out on a Syntex R3 diffractometer with graphite-monochromated Mo Kα radiation. The crystallographic data are summarized in Table I for both crystals.

Table I. Crystallographic Data

	I	II
crystal formula	(C$_{18}$H$_{42}$N$_6$Co)-(C$_4$H$_4$O$_6$)Cl·2H$_2$O	(C$_{18}$H$_{42}$N$_6$Co)-(C$_4$H$_4$O$_6$)Cl·2H$_2$O
a, Å	22.068 (6)	9.666 (3)
b, Å		12.999 (3)
c, Å	10.492 (2)	22.950 (6)
V, Å^3	4426 (2)	2884 (1)
Z	6	4
fw	621.1	621.1
space group	$P6_3$	$P2_12_12_1$
T, °C	20	20
λ, Å	0.71069	0.71069
ρ_{calcd}, g cm^{-3}	1.398	1.431
ρ_{obsd}, g cm^{-3}	1.404	1.433
μ(Mo Kα), cm^{-1}	7.21	7.37
R^a	0.058 (0.061)^c	0.050 (0.059)^c
$R_w{}^b$	0.038	0.049

$^a R = \sum(||F_o| - |F_c||)/\sum|F_o|$. $^b R_w = [\sum w(|F_o| - |F_c|)^2/\sum w(F_o)^2]^{1/2}$. ^{c}Values for the inverted absolute configuration.

The integrated intensities were measured by the ω-scan technique. Three check reflections were monitored after every 197 reflections, and no decay of these reflections was indicated for either crystal. The number of reflection intensities collected was 2770 ($+h,+k,+l$, $3° < 2\theta < 50°$) for I and 3747 ($+h,+k,+l$, $3° < 2\theta < 55°$) for II. Corrections for Lorentz and polarization effects were applied to the intensities, but absorption corrections were not made in view of the small size and uniform shape of both crystals. Extinction corrections were ignored.

Each structure was solved by the conventional heavy-atom method. The crystal structures were refined by the block-diagonal least-squares method using 2206 reflections ($|F_o| > 3\sigma(F_o)$) for I and 3368 reflections

---

[†] Hiroshima University.

[‡] Okayama University of Science.

(1) A recent review: Mason, S. F. *Molecular Optical Activity and the Chiral Discrimination*; Cambridge University Press: Cambridge, U.K., 1982.

(2) For example: Zingg, S. P.; Arnett, E. M.; McPhail, A. T.; Bothner-By, A. A.; Gilkerson, W. R. *J. Am. Chem. Soc.* **1988**, *110*, 1565.

(3) Jeffery, G. A.; Parry, G. S. *Nature (London)* **1952**, *169*, 1105.

(4) Kiosse, G. A. In *Kristallicheskie Structury Neorganicheskikh Soedinenii*; Malinovskii, T. I., Ed. Shtiitsa: Kishinev, USSR, 1974; p 103.

(5) Yoshikawa, Y.; Yamasaki, K. *Coord. Chem. Rev.* **1975**, *28*, 205.

(6) Sakaguchi, U.; Tsuge, A.; Yoneda, H. *Inorg. Chem.* **1983**, *22*, 1630.

(7) Harnung, S. E.; Sorensen, B. S.; Creaser, I.; Maegaard, H.; Pfenninger, U.; Schaffer, C. E. *Inorg. Chem.* **1976**, *15*, 2123.

0020-1669/90/1329-3020$02.50/0

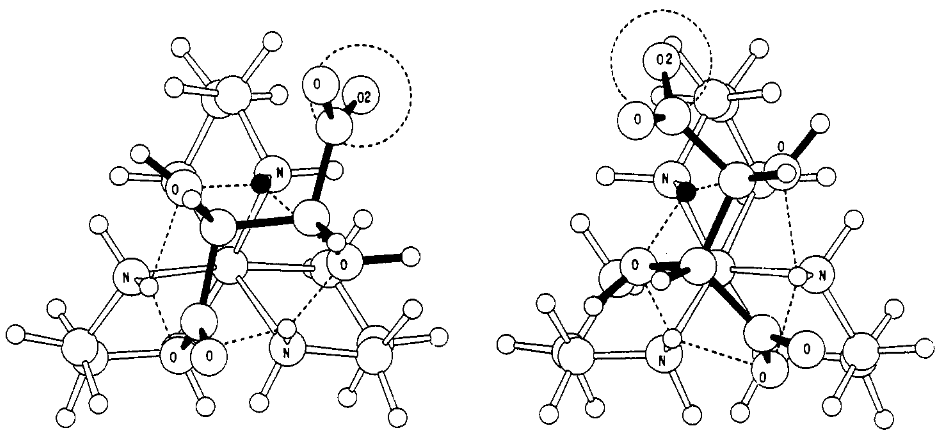

(a) (b)

Figure 1. Typical face-to-face contact modes found in the diastereomeric salts containing *d*-tart^{2-} (indicated in black) and $[Co(en)_3]^{3+}$ ions: (a) Λ-$[Co(en)_3]Br(d\text{-tart})\cdot 5H_2O$;[16] (b) Δ-$[Co(en)_3]_2(d\text{-tart})_3\cdot 11.5H_2O$.[20] The hydroxyl protons are positioned so that the multiple hydrogen bonds are preferably formed with the complex (see text).

for II. The atomic scattering factors were taken from ref 8. After anisotropic refinement of the non-hydrogen atoms, all hydrogen atoms, except those of the water molecules and hydroxyl groups, were assigned idealized positions based on bond distances of 1.09 and 1.00 Å for each C–H and N–H bond, respectively, and a tetrahedral angle around each carbon and nitrogen atom, and the anomalous dispersion coefficients were used for Co and Cl atoms.[8] The final refinement including these hydrogen atoms with isotropic temperature factors converged the R and R_w values to 0.058 and 0.038 for I and 0.050 and 0.049 for II, respectively, where $R = \sum||F_o| - |F_c||/\sum|F_o|$ and $R_w = [\sum w(|F_o| - |F_c|)^2/\sum w|F_o|^2]^{1/2}$. In the refinement, the quantity minimized was $\sum w(|F_o| - k|F_c|)^2$. The weighting scheme used in the final refinement was $w = (\sigma_{cs}{}^2)^{-1}$, where σ_{cs} is the standard deviation obtained from the counting statistics.

All the computations were carried out on a HITAC M-680H computer at the Hiroshima University Information Processing Center. The computer programs used were UNICS-III[9] and ORTEP.[10]

Chromatography. A racemic mixture of *lel*$_3$-$[Co(chxn)_3]^{3+}$ or its related complex ion was absorbed on an SP-Sephadex cation exchanger in a 50-cm length × 1.2-cm diameter column and eluted with aqueous 0.2 M sodium *d*-tartrate. Efficiency of optical resolution attained was visually estimated as a ratio of the elution distances of the two separated bands on the column. Elution orders were determined by the CD spectra of effluents, which were recorded on a Jasco J-40CS spectropolarimeter.

Ab Initio Calculations. Ab initio calculations were carried out for the isolated *d*-tart^{2-} ion by using the GAUSSIAN-82 program[11] with the default analytical-gradient procedure for optimizing molecular structures with a 3-21G basis set[12] employed. All the structure parameters were optimized first for a standard conformer with appropriate dihedral angles, and then the conformational energies were estimated for other conformers with the remaining optimized structure parameters fixed for economy.

Results and Discussion

Background. In the structural study of optical resolution of metal amine complexes, particularly with the *d*-tart^{2-} ion as a resolving reagent, Yoneda et al.[13] have analyzed crystal structures of almost 10 diastereomeric salts of $[Co(en)_3]^{3+}$ and its related complex cations with the *d*-tart^{2-} ion. They found in common a unique face-to-face contact in which the *d*-tart^{2-} ion directs its four almost coplanar oxygen atoms toward the triangular face of the complex ion. The typical contact modes are depicted in Figure 1. When the $[Co(en)_3]^{3+}$ ion has a Λ configuration (Figure 1a), three of the four oxygen atoms, i.e., two alcoholic and one carboxylic oxygen atoms of the *d*-tart^{2-} ion, are nicely placed among three amino protons on the triangular face of the complex, resulting in multiple hydrogen bonds, as shown by broken lines. The fourth oxygen atom (O2), which is of another carboxyl group and which is marked with a broken circle, is then located apart from any part of the complex cation. On the other hand, when the complex has a Δ configuration (Figure 1b), the multiple hydrogen bonds are similarly formed, but the fourth oxygen atom (O2) closely approaches one of the chelate rings of the complex, suffering a steric repulsion. As a result, the *d*-tart^{2-} ion makes a more favorable face-to-face contact with Λ-$[Co(en)_3]^{3+}$ than with its antipode.

Since the above-mentioned face-to-face contact modes have been commonly found in several different diastereomeric salts of $[Co(en)_3]^{3+}$ or its related complex ions with the *d*-tart^{2-} ion, Yoneda et al.[13] proposed that the face-to-face contact is retained also in solution and that it plays an essential role in the chromatographic resolution of these complexes with the *d*-tart^{2-} ion. Consider a tris(diamine)cobalt(III) complex that has a similar triangular face but has bulkier chelate rings than $[Co(en)_3]^{3+}$ does. If this complex adopts a similar association mode with the *d*-tart^{2-} ion, as is expected, more efficient chiral discrimination would be attained. With this expectation in mind, *lel*$_3$-$[Co(chxn)_3]^{3+}$ (chxn = *trans*-1,2-cyclohexanediamine) is chosen as a target complex that meets the above requisites.

X-ray Crystallography. Λ-*lel*$_3$-$[Co(S,S\text{-chxn})_3]Cl(d\text{-tart})\cdot 2H_2O$ (I) was found to be more than 10 times less soluble than its diastereomeric salt, Δ-*lel*$_3$-$[Co(R,R\text{-chxn})_3]Cl(d\text{-tart})\cdot 2H_2O$ (II), in water at ambient temperature, indicating highly efficient chiral discrimination attained in these diastereomeric salts.[14] All atomic coordinates in I and II except for hydrogen atoms are given in Tables II and III, respectively, and those for hydrogen atoms are given in the supplementary material (Tables ST2 and ST3, respectively). The numbering schemes employed for the complex and *d*-tart^{2-} ions in I and II are those given in Figures 4 and 5, respectively. The bond distances and angles for the composite ions in both crystals are in good accord with those reported earlier,[15-22] and they are available also as supplementary material

---

(8) *International Tables For X-ray Crystallography*; Kynoch Press: Birmingham, U.K., 1974; Vol. IV.

(9) Ashida, T. In *The Universal Crystallographic Computation Program System*; Sakurai, T., Ed.; The Crystallographic Society of Japan: Tokyo, 1979.

(10) Johnson, C. K. Report ORNL-3794; Oak Ridge National Laboratory: Oak Ridge, TN, 1976.

(11) Binkley, J. S.; Whiteside, R. A.; Raghavachari, K.; Seeger, R.; DeFrees, D. J.; Schlegel, H. B.; Topiol, S.; Kahn, L. R.; Frisch, M. J.; Fluder, E. M.; Pople, J. A. GAUSSIAN-82 Carnegie-Mellon University, Pittsburgh, PA. We thank the Computer Center, Institute for Molecular Science, Okazaki National Research Institutes, for the use of HITAC-680H and S810/10 computers and Library Program GAUS82.

(12) Binkley, J. S.; Pople, J. A.; Hehre, W. J. *J. Am. Chem. Soc.* **1980**, *102*, 939.

(13) For a review, see: Yoneda, H. *J. Chromatogr.* **1984**, *313*, 59.

(14) Jaerger, F. M.; Bijkerk, L. *Z. Anorg. Allg. Chem.* **1937**, *233*, 97.

(15) Marumo, F.; Utsumi, Y.; Saito, Y. *Acta Crystallogr., Sect. B* **1970**, *26*, 1492.

(16) Kushi, Y.; Kuramoto, M.; Yoneda, H. *Chem. Lett.* **1976**, 135.

(17) Templeton, D. H.; Zalkin, A.; Ruben, H. W.; Templeton, L. K. *Acta Crystallogr., Sect. B* **1979**, *35*, 1608. Magill, L. S.; Korp, J. D.; Bernal, I. *Inorg. Chem.* **1981**, *20*, 1187.

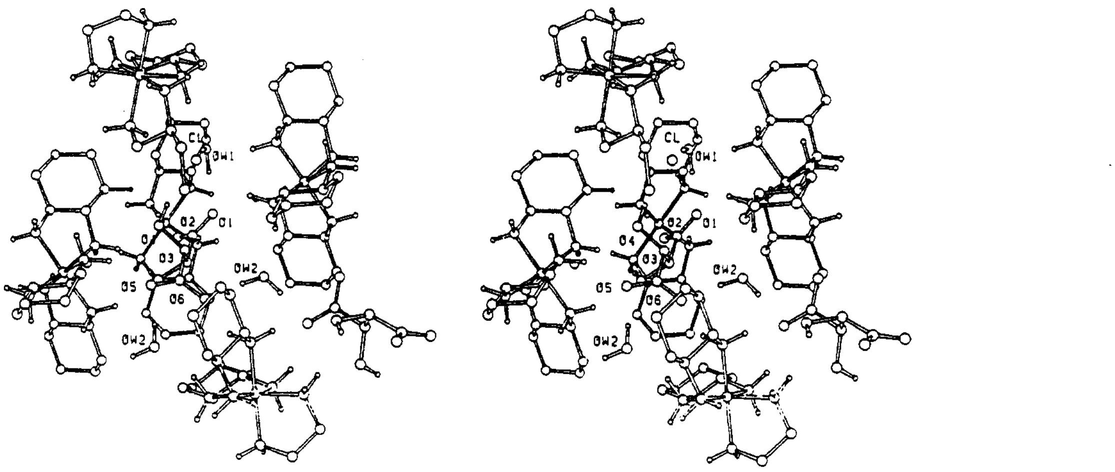

Figure 2. Stereoscopic view of the *d*-tart^{2-} ion surrounded by neighboring ions and water molecules in Λ-*lel*$_3$-[Co(*S*,*S*-chxn)$_3$]Cl(*d*-tart)·2H$_2$O.

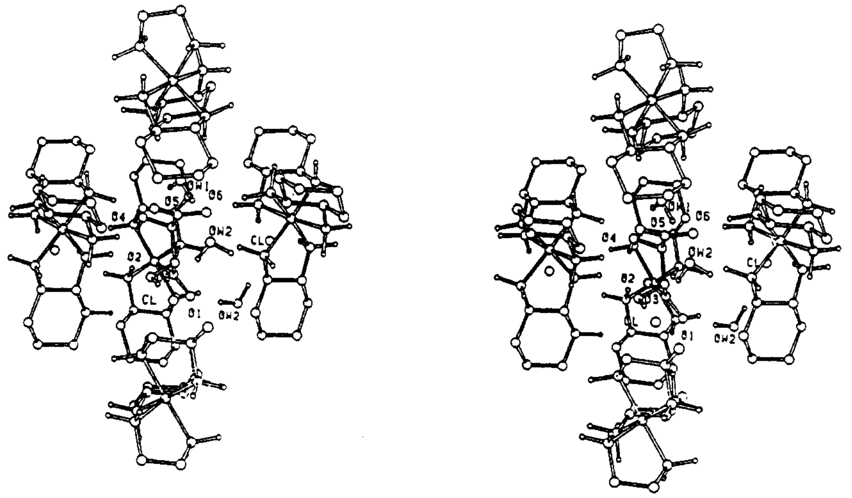

Figure 3. Stereoscopic view of the *d*-tart^{2-} ion surrounded by neighboring ions and water molecules in Δ-*lel*$_3$-[Co(*R*,*R*-chxn)$_3$]Cl(*d*-tart)·2H$_2$O.

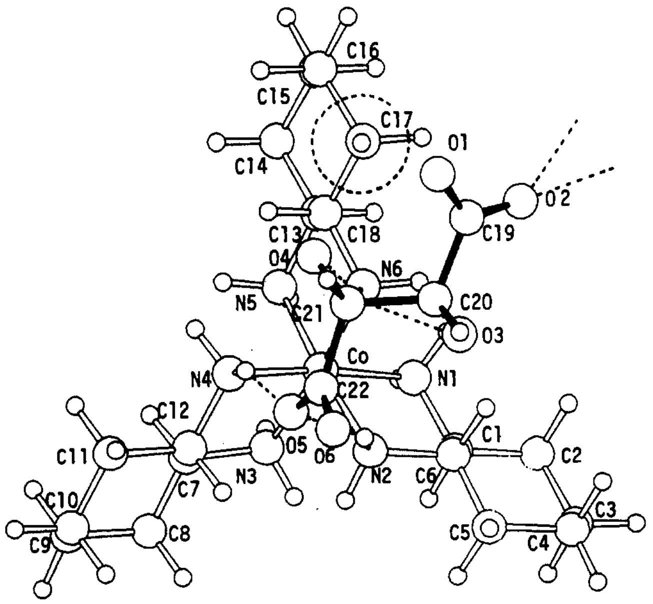

Figure 4. Drawing of the face-to-face contact mode viewed along the C_3 axis of the complex ion with the numbering scheme for Λ-*lel*$_3$-[Co(*S*,*S*-chxn)$_3$]Cl(*d*-tart)·2H$_2$O. Hydrogen bonds are shown by broken lines.

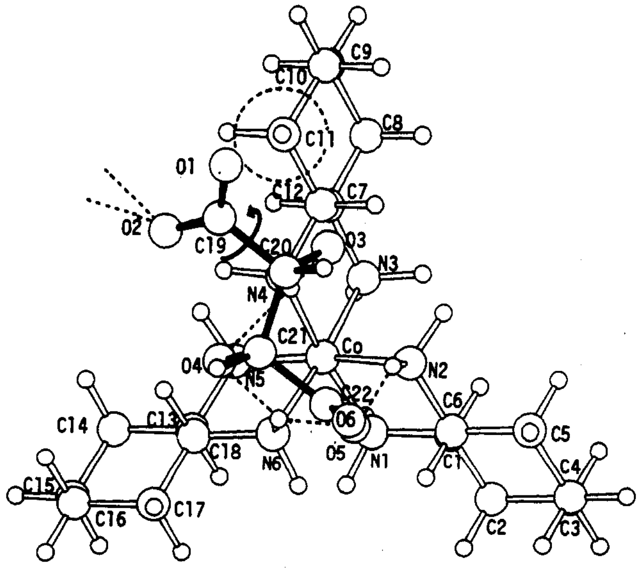

Figure 5. Drawing of the face-to-face contact mode viewed along the C_3 axis of the complex ion with the numbering scheme for Δ-*lel*$_3$-[Co(*R*,*R*-chxn)$_3$]Cl(*d*-tart)·2H$_2$O. Hydrogen bonds are shown by broken lines.

(Tables ST4 and ST5, respectively).

Figures 2 and 3 show how one *d*-tart^{2-} ion is surrounded by neighboring ions and water molecules through hydrogen-bonding in I and II, respectively, where some parts of chelate rings and

---

(18) Tada, T.; Kushi, Y.; Yoneda, H. *Chem. Lett.* **1977**, 379.

(19) Kushi, Y.; Kuramoto, M.; Yoneda, H. *Chem. Lett.* **1976**, 339.

(20) Mizuta, T.; Tada, T.; Kushi, Y.; Yoneda, H. *Inorg. Chem.* **1988**, *27*, 3836.

(21) Okazaki, H.; Sakaguchi, U.; Yoneda, H. *Inorg. Chem.* **1983**, *22*, 1539.

Table II. Atomic Coordinates in Λ-*lel*$_3$-[Co(*S*,*S*-chxn)$_3$]Cl(*d*-tart)·2H$_2$O (I) with Esd's in Parentheses

atom	*x*	*y*	*z*	*B*, Å^2
Co	0.32443 (5)	0.32553 (5)	0.0000 (0)	1.9
N1	0.2612 (3)	0.3500 (3)	−0.0896 (6)	2.5
N2	0.3759 (3)	0.4248 (3)	0.0503 (6)	2.3
N3	0.3814 (3)	0.3418 (3)	−0.1539 (7)	2.8
N4	0.3942 (3)	0.3100 (3)	0.0886 (6)	2.2
N5	0.2663 (3)	0.2269 (3)	−0.0470 (6)	2.5
N6	0.2680 (3)	0.2989 (3)	0.1568 (6)	2.3
C1	0.2966 (4)	0.4279 (4)	−0.1011 (8)	2.5
C2	0.2471 (5)	0.4546 (4)	−0.1383 (9)	3.2
C3	0.2879 (5)	0.5341 (5)	−0.1387 (10)	4.7
C4	0.3228 (5)	0.5630 (4)	−0.0100 (12)	4.6
C5	0.3729 (4)	0.5355 (4)	0.0261 (10)	3.6
C6	0.3307 (4)	0.4562 (4)	0.0276 (8)	2.6
C7	0.4380 (4)	0.3243 (4)	−0.1276 (9)	3.0
C8	0.4997 (5)	0.3593 (5)	−0.2176 (9)	4.3
C9	0.5552 (5)	0.3399 (5)	−0.1751 (11)	5.6
C10	0.5782 (5)	0.3624 (5)	−0.0370 (11)	5.7
C11	0.5150 (4)	0.3265 (5)	0.0520 (9)	3.8
C12	0.4593 (4)	0.3447 (4)	0.0100 (11)	2.7
C13	0.2050 (4)	0.1942 (4)	0.0392 (9)	3.2
C14	0.1665 (5)	0.1144 (4)	0.0348 (11)	5.4
C15	0.1109 (5)	0.0876 (5)	0.1384 (14)	8.2
C16	0.1383 (6)	0.1151 (5)	0.2716 (14)	7.9
C17	0.1752 (5)	0.1954 (5)	0.2713 (11)	4.5
C18	0.2312 (4)	0.2228 (4)	0.1705 (8)	2.7
C19	0.2447 (4)	0.3557 (4)	0.5452 (8)	3.1
C20	0.3139 (4)	0.4020 (4)	0.4778 (9)	2.7
C21	0.3615 (4)	0.3705 (4)	0.4730 (8)	2.7
C22	0.4309 (4)	0.4218 (4)	0.4061 (8)	2.7
O1	0.2466 (3)	0.3261 (3)	0.6457 (5)	4.2
O2	0.1919 (3)	0.3530 (3)	0.4960 (9)	4.8
O3	0.3010 (3)	0.4173 (3)	0.3504 (6)	3.5
O4	0.3261 (3)	0.3030 (3)	0.4107 (5)	3.2
O5	0.4405 (3)	0.4088 (3)	0.2944 (5)	4.1
O6	0.4724 (3)	0.4747 (3)	0.4689 (5)	3.7
Cl	0.1374 (1)	0.3381 (1)	0.1160 (3)	5.0
OW1	0.2001 (4)	0.1909 (4)	−0.2984 (7)	5.9
OW2	0.4376 (3)	0.4794 (3)	−0.2818 (6)	4.1

Table III. Atomic Coordinates in Δ-*lel*$_3$-[Co(*R*,*R*-chxn)$_3$]Cl(*d*-tart)·2H$_2$O (II) with Esd's in Parentheses

atom	*x*	*y*	*z*	*B*, Å^2
Co	0.29793 (7)	0.18680 (5)	0.64880 (3)	1.6
N1	0.2024 (5)	0.2503 (3)	0.5816 (2)	1.8
N2	0.4290 (4)	0.3030 (3)	0.6436 (2)	1.9
N3	0.1691 (4)	0.2601 (3)	0.7015 (2)	1.9
N4	0.3884 (5)	0.1377 (3)	0.7204 (2)	1.9
N5	0.1699 (4)	0.0682 (3)	0.6464 (2)	2.0
N6	0.4190 (4)	0.1025 (3)	0.5987 (2)	1.9
C1	0.2538 (6)	0.3588 (4)	0.5763 (2)	1.9
C2	0.2180 (7)	0.4087 (4)	0.5183 (2)	2.8
C3	0.2820 (8)	0.5161 (5)	0.5149 (3)	3.8
C4	0.4385 (8)	0.5112 (5)	0.5248 (3)	4.2
C5	0.4745 (6)	0.4607 (5)	0.5833 (3)	3.0
C6	0.4103 (6)	0.3538 (4)	0.5856 (2)	2.1
C7	0.1867 (6)	0.2170 (4)	0.7616 (2)	1.9
C8	0.1235 (6)	0.2836 (5)	0.8096 (2)	2.6
C9	0.1554 (7)	0.2374 (5)	0.8692 (2)	3.3
C10	0.3132 (7)	0.2262 (5)	0.8765 (2)	3.8
C11	0.3752 (6)	0.1579 (5)	0.8292 (2)	3.0
C12	0.3412 (5)	0.2033 (4)	0.7698 (2)	2.1
C13	0.2148 (5)	−0.0008 (4)	0.5978 (2)	1.9
C14	0.1491 (7)	−0.1076 (5)	0.6015 (3)	3.0
C15	0.2066 (7)	−0.1768 (5)	0.5533 (3)	3.6
C16	0.3663 (7)	−0.1828 (5)	0.5566 (3)	3.7
C17	0.4300 (6)	−0.0741 (5)	0.5521 (3)	2.8
C18	0.3713 (6)	−0.0057 (4)	0.6009 (2)	2.1
C19	0.7811 (8)	0.0391 (5)	0.7893 (3)	4.1
C20	0.7845 (6)	0.1252 (4)	0.7430 (2)	2.5
C21	0.7815 (6)	0.0790 (4)	0.6812 (2)	2.3
C22	0.8038 (6)	0.1645 (4)	0.6364 (2)	2.2
O1	0.8536 (7)	0.0515 (6)	0.8333 (2)	8.7
O2	0.6977 (6)	−0.0340 (3)	0.7800 (2)	4.8
O3	0.6720 (4)	0.1933 (3)	0.7527 (2)	3.2
O4	0.6518 (4)	0.0278 (3)	0.6720 (2)	2.9
O5	0.7009 (4)	0.2040 (3)	0.6122 (1)	2.7
O6	0.9273 (4)	0.1887 (4)	0.6278 (2)	3.2
Cl	0.7607 (3)	0.4168 (1)	0.7408 (1)	6.2
OW1	0.8142 (6)	0.3455 (3)	0.5290 (2)	4.3
OW2	0.0792 (7)	−0.0421 (5)	0.8803 (2)	7.4

Table IV. Selected Hydrogen-Bond Distances and Angles for Λ-*lel*$_3$-[Co(*S*,*S*-chxn)$_3$]Cl(*d*-tart)·2H$_2$O (I) and Δ-*lel*$_3$-[Co(*R*,*R*-chxn)$_3$]Cl(*d*-tart)·2H$_2$O (II)

O···H–N	O···N, Å	O···H, Å	O···H–N, deg	type
		Crystal I		
O2···H(N4)1–N4	3.098	2.206	148.6	*a*
O2···H(N5)1–N5	2.959	1.958	175.2	*a*
O3···H(N6)2–N6	3.097	2.443	121.8	*b*
O4···H(N6)2–N6	2.938	2.055	144.7	*b*
O5···H(N2)2–N2	3.036	2.139	148.9	*b*
O5···H(N4)2–N4	2.868	1.945	154.6	*b*
		Crystal II		
O2···H(N2)2–N2	3.011	1.986	154.9	*a*
O2···H(N3)2–N3	3.000	1.969	155.8	*a*
O3···H(N4)1–N4	2.930	1.980	143.7	*b*
O4···H(N4)1–N4	3.124	2.316	129.5	*b*
O4···H(N6)1–N6	2.973	2.066	137.2	*b*
O5···H(N2)1–N2	3.014	2.017	149.9	*b*
O5···H(N6)1–N6	3.043	2.100	141.5	*b*

[a] Hydrogen bonds with another neighboring complex. [b] Hydrogen bonds associated with the face-to-face contact.

hydrogen atoms on each carbon atom are eliminated for clarity, but hydrogen atoms on oxygen atoms are positioned appropriately so that they form intimate hydrogen bonds with the neighboring atoms. In both crystals, a familiar face-to-face contact is found in which the *d*-tart^{2-} ion is connected with the complex ion through multiple hydrogen bonds. The contact mode viewed along the C_3 axis of the complex ion is depicted in Figures 4 and 5 for I and II, respectively, and the hydrogen-bond distances and angles relevant to the present discussion are listed in Table IV.

It is evident that the face-to-face contact mode in I is similar to those found commonly in the diastereomeric salts of Λ-[Co(en)$_3$]$^{3+}$ with the *d*-tart^{2-} ion; the three oxygen atoms of the *d*-tart^{2-} ion are hydrogen-bonded to the three amino protons on the triangular face of the complex ion, as indicated by broken lines in Figure 4 (Table IV), and the *d*-tart^{2-} ion assumes a normal conformation usually found. In addition, the distal carboxylate group not involved in the multiple hydrogen bonds to the triangular face is placed far from the bulky chxn chelate rings. A slight difference is discernible in the relative positions of the *d*-tart^{2-} anion and the complex cation between the two contact modes shown in Figures 1a and 4, which is attributed to the hydrogen-bonding of the O2 atom on the distal carboxylate group to another neighboring complex located slightly farther away in I owing to the larger size of the *lel*$_3$-[Co(chxn)$_3$]$^{3+}$ ion.

In the contact mode found in II, the three oxygen atoms of the *d*-tart^{2-} ion are similarly involved in the multiple hydrogen bonds to the complex ion, as indicated by broken lines in Figure 5 (Table IV), and the relative position of the two composite ions is also slightly different from that shown in Figure 1b, which is again due to the hydrogen-bonding of the O2 atom to another neighboring complex. However, a notable difference found between the two contact modes shown in Figures 1b and 5 is the conformation assumed by the *d*-tart^{2-} ion; the *d*-tart^{2-} ion shown in Figure 5 assumes an anomalous conformation in which the distal carboxylate group is rotated considerably, whereas the *d*-tart^{2-} ion in Figure 1b assumes a normal conformation. This suggests that, if the *d*-tart^{2-} ion should assume a normal conformation in II, its distal carboxylate group would suffer a severe steric repulsion imposed on it by the hydrogen atom on one of the chxn chelates, which is depicted in black in Figure 3 and is marked with a broken circle in Figure 5. Actually, the *d*-tart^{2-} ion is forced to rotate

---

(22) Bernal, I.; Korp, J. D.; Creaser, I. I. *Aust. J. Chem.* **1984**, *37*, 2365.

Table V. Conventional Separation Factors Obtained by Chromatographic Resolution[a]

complex	α	K_Λ,[b] M^{-1}	K_Δ,[b] M^{-1}
[Co(en)$_3$]$^{3+}$	1.18	13.3	11.7
[Co(sen)]$^{3+}$	1.18	(71.7)[c]	(49.0)[c]
fac-lel$_3$-[Co(pn)$_3$]$^{3+}$	1.39	30.3	22.5
ob$_3$-[Co(chxn)$_3$]$^{3+}$	1.39	*d*	*d*
lel$_3$-[Co(chxn)$_3$]$^{3+}$	1.57	21.4	15.4

[a] Λ isomers were always eluted first. [b] K_Λ and K_Δ refer to association constants of Λ and Δ isomers, respectively, with *d*-tart^{2-} ion in water at 25 °C.[6] [c] Should not be accepted literally (see text). [d] Not determined.

its distal carboxylate group so as to avoid the steric repulsion. In I, on the other hand, the distal carboxylate group in question is placed apart from the bulky chelate rings (Figures 2 and 4), so that the *d*-tart^{2-} ion can assume a normal and probably energetically more stable conformation, and it makes a favorable face-to-face contact with Λ-*lel*$_3$-[Co(*S,S*-chxn)$_3$]$^{3+}$.

Chromatography. The face-to-face contact modes found in I and II are similar, except for the conformation of the *d*-tart^{2-} ion assumed in II, to those commonly found in several diastereomeric salts of [Co(en)$_3$]$^{3+}$ with the *d*-tart^{2-} ion. It is thus reasonable to presume that the face-to-face contact mode should be retained in solution.[6,21] Therefore, ion-exchange chromatography was applied to the optical resolution of *lel*$_3$-[Co(chxn)$_3$]$^{3+}$ and its related trigonal hexaamine complexes, using aqueous sodium *d*-tartrate as an eluent. The conventional separation factors α estimated from the elution distances are summarized in Table V. It is seen there that both *lel*$_3$-[Co(chxn)$_3$]$^{3+}$ and *fac-lel*$_3$-[Co(pn)$_3$]$^{3+}$ cations are resolved much more efficiently than [Co(en)$_3$]$^{3+}$ is, while the separation factor of [Co(sen)]$^{3+}$ (sen = 1,1,1-tris(((2-aminoethyl)amino)methyl)ethane) is comparable to that of [Co(en)$_3$]$^{3+}$. These results are qualitatively consistent with the diastereomeric association constants of these trigonal complexes with the *d*-tart^{2-} ion, which have been estimated from the CD spectral changes by Sakaguchi et al.[6] and are given also in Table V.

Sakaguchi et al. attributed the higher degree of chiral discrimination attained for the chxn and pn complexes to their conformation fixed to *lel*$_3$. It is highly plausible that those trigonal complexes whose conformation is fixed to *lel*$_3$ have greater association constants[23] because their three amino protons on the triangular face are disposed nicely to form multiple hydrogen bonds with the *d*-tart^{2-} ion. However, more efficient optical resolution attained for *lel*$_3$-[Co(chxn)$_3$]$^{3+}$ than for *fac-lel*$_3$-[Co(pn)$_3$]$^{3+}$, and for *ob*$_3$-[Co(chxn)$_3$]$^{3+}$ than for [Co(en)$_3$]$^{3+}$, cannot be rationalized by the conformational difference alone. We attribute it rather to the difference in the magnitudes of the steric repulsion expected between the distal carboxylate group of the *d*-tart^{2-} ion and one of the chelate rings on the Δ enantiomers of these complexes. It is then natural that *lel*$_3$-[Co(chxn)$_3$]$^{3+}$ should be resolved more efficiently than *fac-lel*$_3$-[Co(pn)$_3$]$^{3+}$ is and much more than [Co(en)$_3$]$^{3+}$ or [Co(sen)]$^{3+}$ is because the former Δ complex has a bulkier substituent on each chelate ring, imposing a more severe steric repulsion on the distal carboxylate group, and because the latter two complexes have practically no substituents on the en chelate rings. In addition, molecular model consideration indicates that the *d*-tart^{2-} ion experiences a similar but smaller steric repulsion from Δ-*ob*$_3$-[Co(*S,S*-chxn)$_3$]$^{3+}$[24] than from Δ-*lel*$_3$-[Co(*R,R*-chxn)$_3$]$^{3+}$ in the face-to-face contact mode. In this way, all the chromatographic data in Table V are readily and reasonably interpreted.

It is notable in Table V that fairly large association constants K_Λ and K_Δ have been obtained for [Co(sen)]$^{3+}$ and that the high K_Λ/K_Δ ratio seems to ensure the attainment of efficient optical resolution for [Co(sen)]$^{3+}$. However, its separation factor and retention volume actually found are both comparable to those of [Co(en)$_3$]$^{3+}$, in conflict with the association constants obtained by Sakaguchi et al.[6] The discrepancy is attributed to undue assumptions made to determine the K_Λ and K_Δ values by CD spectral measurements, as pointed out earlier,[25] and thus these values should not be accepted literally.

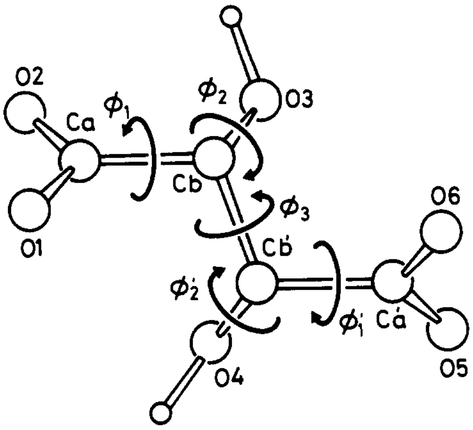

Figure 6. Definition of conformational angles in the *d*-tart^{2-} ion. A hydrogen atom on each carbon atom is eliminated for clarity.

Table VI. Conformational Angles of the *d*-Tartrate Anion

	conformational angles, deg			
salt	ϕ_1	ϕ_1'	ϕ_3	ref
Λ-[Co(en)$_3$]Br(*d*-tart)·5H$_2$O	15.6	18.5	176.0	16
Λ-[Co(en)$_3$]Cl(*d*-tart)·5H$_2$O	15.6	19.4	177.9	17
Λ-[Co(en)$_3$](*d*-tartH)(*d*-tart)·3H$_2$O	4.4	1.4	184.6	18
Li[Λ-[Cr(en)$_3$](*d*-tart)$_2$]·3H$_2$O	13.4	6.9	178.2	19
Δ,Λ-[Co(en)$_3$]$_2$(*d,l*-tart)$_3$·10H$_2$O				20
tartrate 1[a]	3.8	13.2	178.7	
tartrate 2[b]	6.3	12.1	182.7	
tartrate 3[a]	12.7	16.8	180.2	
Λ-[Co(en)$_3$]$_2$(*d*-tart)$_3$·19H$_2$O				20
tartrate 1	10.8	19.3	183.3	
tartrate 2	0.8	16.1	182.0	
tartrate 3	14.2	10.2	183.4	
Δ-[Co(en)$_3$]$_2$(*d*-tart)$_3$·11.5H$_2$O				20
tartrate 1	2.8	15.3	182.7	
tartrate 3	14.2	12.5	184.8	
Λ-[Co(sen)]Cl(*d*-tart)·6H$_2$O	11.2	23.0	179.3	21, 22
Δ-[Co(sen)]Cl(*d*-tart)·4.5H$_2$O	5.1	15.4	178.7	22
Λ-[Co(chxn)$_3$]Cl(*d*-tart)·2H$_2$O	−16.4	16.9	181.2	this work
Δ-[Co(chxn)$_3$]Cl(*d*-tart)·2H$_2$O	81.2	24.9	187.2	this work

[a] Δ (Λ) complex with the *d*-tart^{2-} (*l*-tart^{2-}) ion. [b] Λ (Δ) complex with the *d*-tart^{2-} (*l*-tart^{2-}) ion.

Conformation of the *d*-Tartrate Ion. In order to examine the anomalous conformation assumed by the *d*-tart^{2-} ion in II, its conformational angles are defined as shown in Figure 6. Oxygen atoms O2, O3, O4, and O5 are those facing toward the complex ion, and of these, O3, O4, and O5 are hydrogen-bonded to the amino protons on the triangular face of the complex. When the Ca–O2 (Ca'–O5) bond is eclipsed with the Cb–O3 (Cb'–O4) bond, ϕ_1 (ϕ_1') is set equal to 0°. ϕ_2 (ϕ_2') is 0° when the O3–H (O4–H) bond is eclipsed with the Cb–Ca (Cb'–Ca') bond, and ϕ_3 is 180° when the two carboxylate groups are trans to each other. Each arrow in Figure 6 denotes a positive direction. In Table VI are listed the dihedral angles ϕ_1, ϕ_1', and ϕ_3 thus defined and actually found in I and II and other relevant diastereomeric salts.[16-22]

It is notable first in Table VI that the angle ϕ_3 is very close to 180° for each *d*-tart^{2-} ion, consistent with a generally accepted claim that two carboxylate groups are always trans to each other in a *d*-tart^{2-} ion.[4,26] Second, each *d*-tart^{2-} ion also has a similar ϕ_1' angle, which determines the orientation of the carboxylate group hydrogen-bonded to the triangular face of the complex,

---

(23) Ogino, K. *Bull. Chem. Soc. Jpn.* **1969**, *42*, 447. Yoneda, H.; Miyoshi, K.; Matsukawa, H. *Bull. Chem. Soc. Jpn.* **1982**, *55*, 1969.

(24) Kobayashi, A.; Marumo, F.; Saito, Y. *Acta Crsystallogr., Sect. C* **1983**, *39*, 807.

(25) Miyoshi, K.; Izumoto, S.; Nakai, K.; Yoneda, H. *Inorg. Chem.* **1986**, *25*, 4654.

(26) Ascenso, J.; Gil, V. M. S. *Can. J. Chem.* **1980**, *58*, 1376.

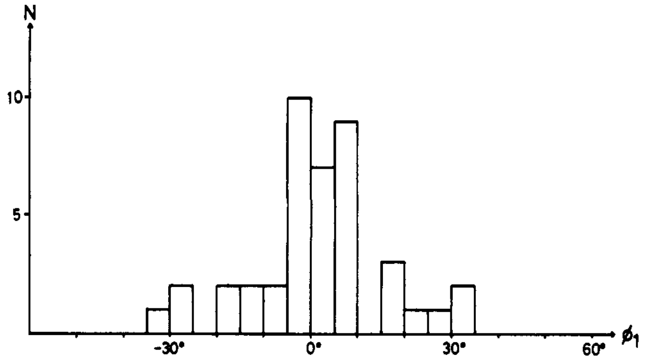

Figure 7. Distribution of the conformational angle ϕ_1 in simple salts of d-tart^{2-} and d-tartH$^-$ ions. Note that ϕ_1' is indistinguishable from ϕ_1 in these salts so that both are treated equivalently.

indicating that the d-tart^{2-} ion forms favorable multiple hydrogen bonds to it at that ϕ_1' angle (ca. 16° on average). Somewhat different ϕ_1' angles found in Λ-[Co(en)$_3$](d-tart)(d-tartH)·3H$_2$O and Li[Λ-[Cr(en)$_3$](d-tart)$_2$]·3H$_2$O are attributed to the fact that it is the d-tartH$^-$ or d-tartLi$^-$ ion but not the d-tart^{2-} ion that is making a face-to-face contact in these salts.[18,19] Similarly, both Λ-[Co(sen)]Cl(d-tart)·6H$_2$O and II have ϕ_1' angles different to some extent from others (Table VI), which is probably due to the hydrogen-bonding of the O6 atom to the neighboring water molecules in the former[21,22] and to the amino protons on the triangular face of another neighboring complex in II (Figure 3).

Finally, it is notable in Table VI that the angle ϕ_1 in II is exceptionally large, while each d-tart^{2-} ion in other crystals has a comparable ϕ_1 angle (ca. 9° on average). In other words, the d-tart^{2-} ion in II takes an unprecedented conformation in which one of the carboxylate groups is rotated by as much as 80° around the Ca–Cb bond with other dihedral angles almost unchanged. A close inspection of Figures 3 and 5 reveals that the ϕ_1 angle of 81.2° is much larger than is needed just to avoid the steric repulsion from the chelate ring. How anomalous the ϕ_1 angle of 81.2° is, is recognized from the distribution of the ϕ_1 angles of d-tart^{2-} and d-tartH$^-$ ions found in their simple salts (Figure 7).[27] In contrast, the d-tart^{2-} ion in I takes a conformation close to those commonly encountered except for its ϕ_1 angle of −16.4° (vide infra). Then, it is essential to estimate the energy required to rotate the carboxylate group, in order to search for the factors leading to highly efficient chiral discrimination attained for the lel_3-[Co(chxn)$_3$]$^{3+}$–d-tart^{2-} system.

Ab Initio Calculations. Ab initio molecular orbital calculations were carried out to estimate the rotational barrier of the carboxylate group in the d-tart^{2-} ion making a face-to-face contact with [Co(en)$_3$]$^{3+}$-type trigonal hexaamine complexes. A starting conformer is selected so that it has average structure parameters for most of the d-tart^{2-} ions listed in Table VI; Λ-[Co(en)$_3$](d-tart)(d-tartH)·3H$_2$O, Li[Λ-[Cr(en)$_3$](d-tart)$_2$]·3H$_2$O, and the last two salts were omitted in averaging because of their unusual ϕ_1 and/or ϕ_1' angles (vide supra). The starting conformer thus selected has the following dihedral angles: ϕ_1 = 9°, ϕ_1' = 16°, ϕ_3 = 180°.

The remaining dihedral angles ϕ_2 and ϕ_2' were selected so that the d-tart^{2-} ion could direct the lone-pair electrons on its O3 or O4 atom so as to form the most favorable multiple hydrogen bonds to the complex and to suffer the minimum electrostatic repulsion on its hydroxyl protons from the amino protons on the triangular face of the complex, as shown in Figure 1. The ϕ_2 and ϕ_2' angles thus selected were 60 and 100°, respectively, which are close to those actually found in some diastereomeric salts: ϕ_2 = 58.9° and ϕ_2' = 107.4° in Λ-[Co(en)$_3$]Br(d-tart)·5H$_2$O,[16] ϕ_2 = 65.9° and ϕ_2' = 100.8° in Λ-[Co(en)$_3$]Cl(d-tart)·5H$_2$O,[17] and ϕ_2 = 72.8° and ϕ_2' = 90.4° in Λ-[Co(sen)]Cl(d-tart)·6H$_2$O.[21] The corresponding angles have not been reported in other relevant salts.

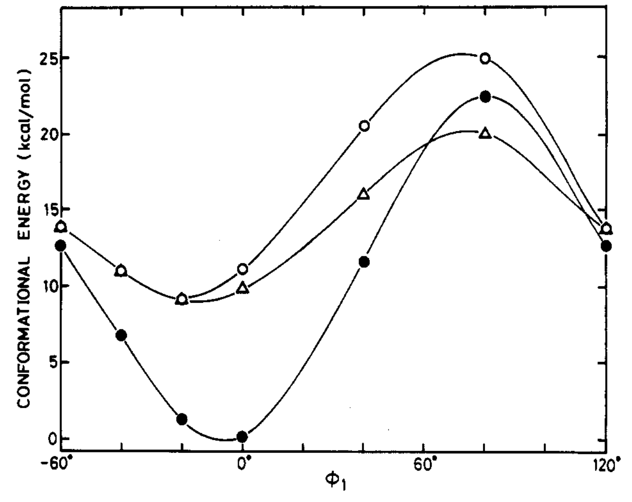

Figure 8. Variation of the conformational energy of the d-tart^{2-} ion with the ϕ_1 angle for ϕ_2 = 0° (●), ϕ_2 = 60° (○), and ϕ_2 = 180° (△). Note that other angles ϕ_1', ϕ_2', and ϕ_3 are fixed to 16, 100, and 180°, respectively.

Structural optimization was carried out first for our starting conformer defined above with all of its dihedral angles fixed (ϕ_1 = 9°, ϕ_1' = 16°, ϕ_2 = 60°, ϕ_2' = 100°, and ϕ_3 = 180°), and the structure parameters thus obtained were satisfactory ones. Conformational energies were then calculated with the ϕ_1 angle varied but with all other parameters fixed, since our attention is focused primarily on the rotational barrier of the distal carboxylate group. Similar calculations were carried out for ϕ_2 = 0° and ϕ_2 = 180° as well, since, when ϕ_2 = 0°, the internal hydrogen-bonding is possible between carboxylate and hydroxyl groups on the same carbon atom, and it contributes to the stabilization of the d-tart^{2-} ion,[28] but it is completely impossible for any ϕ_1 angle when ϕ_2 = 180°. The relative energies thus obtained are plotted in Figure 8 for ϕ_2 = 0, 60, and 180° as a function of ϕ_1.

Figure 8 clearly indicates that the d-tart^{2-} ion is the most stable when ϕ_1 = 0° for ϕ_2 = 0°, and the energy minimum is found around ϕ_1 = −20° for both ϕ_2 = 60° and ϕ_2 = 180°, while the energy maximum is found always around ϕ_1 = 80°. In other words, it is confirmed that the d-tart^{2-} ion is stable when all of the oxygen and carbon atoms in each α-hydroxy carboxylate group lie roughly on the same plane, i.e., when $\phi_1 \simeq 0°$, while the rotation of the carboxylate group leads to considerable destabilization of the isolated d-tart^{2-} ion. These results are in good agreement with those obtained by Newton and Jeffrey[29] and Gunthard et al.,[30] who carried out similar calculations on glycolic acid, glycolate anion, and glycolaldehyde. The conclusion they drew is that it is due to an intrinsic property of the C(OH)—C═O group and to the internal hydrogen-bonding that α-hydroxy carboxylic acids prefer a planar conformation.

Mechanism of Chiral Discriminiation. Now, our attention is focused on the conformation of the d-tart^{2-} ion making a face-to-face contact with [Co(en)$_3$]$^{3+}$. It is certain in Figure 8 that the d-tart^{2-} ion itself is more stable when ϕ_2 = 0° than when ϕ_2 = 60° for any ϕ_1 angle, which is at least in part attributed to the internal hydrogen bond formed favorably for the conformer with ϕ_2 = 0°.[28-30] However, the fact that the d-tart^{2-} ion actually assumes a conformation with ϕ_2 = 60° in some diastereomeric salts of [Co(en)$_3$]$^{3+}$ suggests that the conformational energy loss for ϕ_2 = 60° must be fully compensated by the face-to-face multiple hydrogen-bonding to the complex, which is formed more

---

[27] Data on the ϕ_1 (ϕ_1') angles were taken from the Cambridge Crystallographic Data File (CCDF) up to 1986. The criterion for accepting an entry from the CCDF was that no atom heavier than calcium should be present in the structure so that C, O, and H atoms could be well located.

[28] Polavarapu, P. L.; Ewig, C. S.; Chandramouly, T. *J. Am. Chem. Soc.* **1987**, *109*, 7382.

[29] Newton, M. D.; Jeffery, G. A. *J. Am. Chem. Soc.* **1977**, *99*, 2413.

[30] Ha, T.-K.; Blom, C. E.; Gunthard, H. H. *J. Mol. Struct.* **1981**, *85*, 285. Hollenstein, H.; Ha, T.-K.; Gunthard, H. H. *J. Mol. Struct.* **1986**, *146*, 289.

favorably for the conformer with $\phi_2 = 60°$, as mentioned above.

The ϕ_1 angle actually adopted in the diastereomeric salts of $[Co(en)_3]^{3+}$ varies in the range from 0 to 15° (Table VI), which deviates somewhat from the ideal angle of −20° for $\phi_2 = 60°$. However, the energy loss relative to the ideal conformation amounts only to 2.0 kcal/mol for $\phi_1 = 0°$ and 5.3 kcal/mol for $\phi_1 = 15°$ (Figure 8), which is probably supplied by the electrostatic interaction possible between the O2 atom marked with a broken circle and one of the amino protons (shown in black) on the complex (Figure 1); the attractive interaction becomes progressively effective as the ϕ_1 angle changes from −20° to a certain positive angle, e.g., to the maximum ϕ_1 angle of 15.6° actually found. Consequently, it is safely concluded that the conformer found in the diastereomeric salts of $[Co(en)_3]^{3+}$ is not energetically unstable.

Next, turning to the conformation of the *d*-tart^{2-} ion in I and II, the ϕ_2 (ϕ_2') angle has not been determined in either crystal because of uncertainty in the position of the hydroxyl proton. The *d*-tart^{2-} ion may adopt the ϕ_2 angle of 60°, or it may adopt the ϕ_2 angle of 0° to form the internal hydrogen bond at the expense of the multiple hydrogen bonds to the complex, since the O3 atom is placed somewhat unfavorably for the multiple hydrogen bonds in both crystals, as pointed out earlier. However, whichever ϕ_2 angle the *d*-tart^{2-} ion may adopt, much energy must be dissipated to rotate the carboxylate group by as much as 80°, where it is the most destabilized (Figure 8). Therefore, it follows that the conformer with $\phi_1 = 80°$ found in II suffers considerable destabilization which, we propose, is mainly responsible for a remarkable solubility difference between I and II.

The destabilization of the *d*-tart^{2-} ion in II is of course compensated greatly by the hydrogen-bonding with the neighboring molecules; overall hydrogen-bonding interactions are actually stronger in II, as judged from higher density and greater number of hydrogen bonds present in II than in I (see Tables I, ST1, ST6, and ST7). In particular, the double hydrogen bonds of the O2 atom to another neighboring complex come into play and contribute to the stabilization when the carboxylate group is rotated considerably. This is probably why the *d*-tart^{2-} ion rotates the carboxylate group by a much greater angle than is needed just to avoid the steric repulsion in II. Furthermore, structural optimization carried out with ϕ_1, ϕ_1', ϕ_2, ϕ_2', and ϕ_3 angles fixed to 80, 16, 60, 100, and 180°, respectively, leads to additional stabilization of ca. 3.6 kcal/mol for this conformer. In addition, though the ϕ_2' angle was above set equal to 100°, it might be much greater than 100° in II, because the O2 atom in the rotated carboxylate group approaches the O4 atom to form another type of internal hydrogen bond to its proton,[28] which is best formed when $\phi_2' =$ ca. 200° (Figure 3). If such an interaction takes place, the conformer with a ϕ_1 angle of 80° will be further stabilized. Therefore, the actual free energy difference estimated from the solubility difference between I and II may well be much lower than the destabilization energy calculated for the isolated *d*-tart^{2-} ion with $\phi_1 = 80°$.

The conformer found in I has a ϕ_1 angle of −16.4°, which differs somewhat from the average ϕ_1 angle of 9°, as pointed out earlier. This may be due to the hydrogen-bonding of the O2 atom to the two amino protons of another neighboring complex and also due to the weak steric repulsion expected between the O2 atom and the hydrogen atom, which is depicted in black in Figure 2 and is marked with a broken circle in Figure 4.

Finally, let us consider a conformation of the *d*-tart^{2-} ion associated with the *lel*$_3$-$[Co(chxn)_3]^{3+}$ ion in solution. Since the face-to-face contact modes found in I and II are fairly similar, with respect to the multiple hydrogen bonds with the complex, to those commonly found, they are probably retained in solution.[6,21] However, the *d*-tart^{2-} ion will not rotate the distal carboxylate group when it makes a face-to-face contact with Δ-*lel*$_3$-[Co(*R*,*R*-chxn)$_3$]$^{3+}$ in solution, because another neighboring complex is absent in solution that would serve to compensate the high rotational barrier of the carboxylate group. Therefore, the *d*-tart^{2-} ion experiences a steric repulsion from the bulky chelate ring of Δ-*lel*$_3$-[Co(*R*,*R*-chxn)$_3$]$^{3+}$, and thus the multiple hydrogen bonds are more or less damaged so as to avoid the steric repulsion, whereas favorable multiple hydrogen bonds are possible with Λ-*lel*$_3$-[Co(*S*,*S*-chxn)$_3$]$^{3+}$, which is mainly responsible for the much higher degree of optical resolution attained for *lel*$_3$-$[Co(chxn)_3]^{3+}$ by chromatography. A similar explanation applies to *lel*$_3$-$[Co(pn)_3]^{3+}$, but since the steric repulsion expected is less severe, the degree of optical resolution attainted for it is lower than for *lel*$_3$-$[Co(chxn)_3]^{3+}$.

In conclusion, the *d*-tart^{2-} ion has a strong tendency to maintain a planar conformation at each α-hydroxy carboxylate group, which is ultimately responsible for the highly efficient chiral discrimination attainted by the *d*-tart^{2-} ion for *lel*$_3$-$[Co(chxn)_3]^{3+}$ both in the solid state and in solution.

Supplementary Material Available: Full listings of the crystallographic data I and II (Table ST1), hydrogen atom coordinates for I and II (Tables ST2 and ST3, respectively), all bond distances and angles for I and II (Tables ST4 and ST5, respectively), hydrogen-bond distances and angles for I and II (Tables ST6 and ST7, respectively), and thermal parameters for I and II (Tables ST8 and ST9, respectively) (15 pages); listings of observed and calculated structure factor amplitudes for I and II (Tables ST10 and ST11, respectively) (14 pages). Ordering information is given on any current masthead page.